Steady-State Computations Using Summation-by-Parts Operators

Magnus Svärd, Ken Mattsson and Jan Nordström

Tweet

LINKÖPING UNIVERSITY

Steady-State Computations Using Summation-by-Parts Operators

Magnus Svärd,[1] **Ken Mattsson,**[2] **and Jan Nordström**[3]

This paper concerns energy stability on curvilinear grids and its impact on steady-state calulations. We have done computations for the Euler equations using fifth order summation-by-parts block and diagonal norm schemes. By imposing the boundary conditions weakly we obtain a fifth order energy-stable scheme. The calculations indicate the significance of energy stability in order to obtain convergence to steady state. Furthermore, the difference operators are improved such that faster convergence to steady state are obtained.

KEY WORDS: High order finite differences; summation-by-parts operators; convergence to steady state; stability.

1. INTRODUCTION

Previously, our focus has been on time dependent problems where high-order methods are necessary to accurately compute fine structures of the flow. (see [1–3]) However, those methods need good steady-state solutions as initial data which shifted our focus towards computation of such solutions. In this paper we address some key issues relevant to the efficient and accurate computation of steady state solutions by using high-order finite difference methods.

There are a variety of methods to speed up convergence to steady-state but the interest here is on properties of the finite difference methods themselves. If a difference method have bad properties, convergence

[1] Department of Information Technology, Uppsala University, Uppsala, Sweden. E-mail: magnuss@tdb.uu.se

[2] Department of Information Technology, Uppsala University, Uppsala, Sweden.

[3] The Swedish Defence Research Agency, Division of Systems Technology, Department of Computational Physics, SE-164 90 Stockholm, Sweden and Department of Information Technology, Uppsala University, Uppsala, Sweden.

to the correct solution will not be possible regardless of any convergence acceleration techniques. For this reason only local time stepping is used to enhance convergence to steady-state.

In [4] and [5] summation-by-parts (SBP) operators were developed for Cartesian grids. These operators makes it possible to prove stability using energy estimates. However, in [6] it was shown that stability might be destroyed when a general SBP operator is applied to curvilinear grids and stability is only recovered for a certain class of SBP operators.

Recently, SBP conserving dissipation operators were developed, (see [7]). These are of the same order of accuracy as the scheme itself, but can also be used to construct upwind schemes with the proper scaling. In the upwind case, one order of accuracy less is obtained.

Further, in [8–11] a theory for imposing boundary conditions weakly using SBP operators with a simultaneous approximation term (SAT) is developed. The SAT boundary procedure can be used both for external and internal boundaries, making the scheme stable for grids composed of blocks. Moreover, this technique gives a straightforward way of efficient parallelization.

The technique mentioned above was used to construct fifth order accurate upwind schemes, which were used to compute steady state solutions to the Euler equations around a NACA0012 airfoil. Both the non-energy stable SBP schemes applied to curvilinenar grids as well as the energy stable schemes are used and compared to each other. To speed up convergence to steady state, the difference operators are modified in order to give the smallest spectral radius. Also, as was mentioned above, local time stepping is used.

The contents of this report are divided as follows: In Sec. 2, the Euler equations and the flux splitting employed, are given; Sec. 3 displays the discretization techniques and also an explanation of the parallel implementation; numerical experiments are performed in Sec. 4. In Sec. 5 conclusions are drawn.

2. THE CONTINUOUS PROBLEM

2.1. Governing Equations

The Euler equations in curvilinear coordinates, $x = x(\xi, \eta)$ and $y = y(\xi, \eta)$, become,

$$
\begin{pmatrix} J\rho \\ J\rho u \\ J\rho v \\ J\rho(e + \frac{V^2}{2}) \end{pmatrix}_t + \begin{pmatrix} J\rho(\xi_x u + \xi_y v) \\ J\rho u(\xi_x u + \xi_y v) + J\xi_x p \\ J\rho v(\xi_x u + \xi_y v) + J\xi_y p \\ J(\rho(e + \frac{V^2}{2}) + p)(\xi_x u + \xi_y v) \end{pmatrix}_\xi
$$

$$+ \begin{pmatrix} J\rho(\eta_x u + \eta_y v) \\ J\rho u(\eta_x u + \eta_y v) + J\eta_x p \\ J\rho v(\eta_x u + \eta_y v) + J\eta_y p \\ J(\rho(e + \frac{V^2}{2}) + p)(\eta_x u + \eta_y v) \end{pmatrix}_\eta = \begin{pmatrix} 0 \\ 0 \\ 0 \\ 0 \end{pmatrix},$$

where $J = (\xi_x \eta_y - \xi_y \eta_x)^{-1}$; ρ is the density; u, v are the velocity components in the x, y directions, respectively; e denotes the internal energy and p the pressure. A complete derivation of these equations is found in [11].

2.2. Lax–Friedrich Flux Splitting

We will formulate the two-dimensional Euler equations using the Lax–Friedrich flux splitting formulation. Consider the 2-D system with m unknowns,

$$\mathbf{u}_t + \mathbf{F}_x + \mathbf{G}_y = 0, \quad a \leqslant x \leqslant b, \quad c \leqslant y \leqslant d, \tag{1}$$

where $\mathbf{u}$ is the solution vector and $\mathbf{F} = \mathbf{A}\mathbf{u}$ and $\mathbf{G} = \mathbf{B}\mathbf{u}$ are the flux vectors. The matrices $\mathbf{A}$ and $\mathbf{B}$ are the flux Jacobian matrices. We start by splitting the flux vectors into two parts with positive and negative running characterists respectively. We obtain $\mathbf{F} = \mathbf{A}\mathbf{u} = \frac{1}{2}(\mathbf{A} + \alpha\, I_m)\mathbf{u} + \frac{1}{2}(\mathbf{A} - \alpha\, I_m)\mathbf{u} = \mathbf{A}_+\mathbf{u} + \mathbf{A}_-\mathbf{u}$ and $\mathbf{G} = \mathbf{B}\mathbf{u} = \frac{1}{2}(\mathbf{B} + \beta\, I_m)\mathbf{u} + \frac{1}{2}(\mathbf{B} - \beta\, I_m)\mathbf{u} = \mathbf{B}_+\mathbf{u} + \mathbf{B}_-\mathbf{u}$, where α and β are the largest eigenvalues, in magnitude, to $\mathbf{A}$ and $\mathbf{B}$, respectively and I_m is the $m \times m$ identity matrix. The system (1) can now be written as

$$\mathbf{u}_t + (\mathbf{A}_+\mathbf{u})_x + (\mathbf{A}_-\mathbf{u})_x + (\mathbf{B}_+\mathbf{u})_x + (\mathbf{B}_-\mathbf{u})_y = 0. \tag{2}$$

These fluxes will be discretized with upwind and downwind finite difference operators.

3. COMPUTATIONAL PROCEDURE

We use numerical schemes with an SBP property for stability reasons. The summation-by-parts properties are the following for the first derivative: let h denote the spacing between two grid points. Further, let the grid consist of $N + 1$ points numbered from 0 to N. Let u denote a grid function and u_x denote its exact derivative projected onto the same grid. Denote by $P^{-1}Q$ an $2m$th order accurate approximation of the first derivative operator,

$$P^{-1}Qu = u_x + [\mathcal{O}(h^{2m-1}), \ldots, \mathcal{O}(h^{2m-1}), \mathcal{O}(h^{2m}), \ldots]^T. \tag{3}$$

The operator $P^{-1}Q$ is an SBP operator if (i) the matrix P is symmetric and positive definite and defines a norm $\|u\|_P^2 = u^T P u$ and (ii) the matrix Q is nearly skew-symmetric and $Q + Q^T = B$, where B is diagonal such that $B = \mathrm{diag}[-1, 0, \ldots, 0, 1]$. To obtain the accuracy stated in (3), P is diagonal except at the upper left and lower right corners which contains blocks. P is then called a block norm. If P is diagonal it is called a diagonal norm. Although, it is an abuse of language we will use the word norm to describe a matrix P when we mean that P defines a norm through $\|u\|_P^2 = u^T P u$.

3.1. Stability on Curvilinear Grids

The SBP operator above is valid only on equidistant Cartesian grids. Below we will give the conditions for stability on curvilinear grids. The details are found in [6]. Let $\xi(x)$ be a transformation between the x-coordinate and ξ-coordinate and let $x(\xi)$ be the inverse transformation. Consider the advection equation,

$$v_t + v_x = 0, \quad t \geqslant 0, \quad a \leqslant x \leqslant b, \text{ or,} \tag{4}$$

$$x_\xi v_t + v_\xi = 0, \quad t \geqslant 0, \quad 0 \leqslant \xi \leqslant 1, \tag{5}$$

since $\xi_x^{-1} = x_\xi$ and $\xi(a) = 0$, $\xi(b) = 1$.

The energy rate for Eq. (4) is obtained by multiplying by v and integrating over x,

$$\frac{d}{dt}\|v\|^2 = (v(a, t))^2 - (v(b, t))^2. \tag{6}$$

Equation (5) is discretized on $[0, 1]$ with $n + 1$ equidistant points indexed from 0 to n. Let the matrix X_ξ^d be such that, $(X_\xi^d)_{ii} = x_\xi(i \Delta \xi)$, $i = 0 \ldots n$, on the diagonal and 0 elsewhere. Let u be the approximate solution to v in each grid point, $u(t) = [u_0(t), u_1(t), \ldots, u_n(t)]^T$. Then the discretized version of Eq. (5) becomes,

$$X_\xi^d u_t + P^{-1}Q u = 0, \tag{7}$$

where $P^{-1}Q$ is the difference operator on an equidistant grid previously defined.

In the same manner as in the continuous case, Eq. (7) is multiplied by $u^T P$ to acquire,

$$u^T P X_\xi^d u_t + u^T Q u = 0.$$

Adding the transpose yields,

$$u^T P X_\xi^d u_t + u_t^T (P X_\xi^d)^T u + u^T (Q + Q^T) u = 0. \tag{8}$$

In general, $P X_\xi^d$ is neither positive definite nor symmetric. Hence, the first two terms in Eq. (8) do not form a total derivative. Thus (8) does not lead to an energy estimate. If $P X_\xi^d$ could be modified to a symmetric norm, $P X_\xi$, Eq. (8) would be,

$$\frac{d}{dt}(u^T P X_\xi u) + u^T (Q + Q^T) u = 0, \quad \text{or} \quad \frac{d}{dt}||u||_{P X_\xi}^2 = u_0^2 - u_n^2. \tag{9}$$

i.e. an equation similar to Eq. (6). Note that if P is diagonal matrix, $P X_\xi^d$ would indeed be a norm since a valid coordinate transformation X_ξ^d is positive definite and diagonal by construction. In fact, this is the only choice to obtain an energy estimate as is shown in [6]. If P is diagonal the boundary can only be closed at half the internal accuracy such that,

$$P^{-1} Q u = u_x + [\mathcal{O}(h^m), \ldots, \mathcal{O}(h^m), \mathcal{O}(h^{2m}), \ldots]^T. \tag{10}$$

The global accuracy is then reduced to $m + 1$. However, as will be shown in the next subsection, the loss of efficiency is only minor in the context of upwind operators.

3.2. Artificial Dissipation and Upwind Operators

For non-linear convection problems it is well known that centered difference schemes require the addition of artificial dissipation to absorb the energy of the unresolved modes. Further, in the previous subsection we claimed that diagonal norms are necessary on non-equidistant grids for stability reasons. If we want to compute a solution with a fifth order method we have to use an eighth order internal scheme with a fourth order boundary closure. Thus, the internal scheme is unnecessary accurate and wide. However, for the above mentioned stability reasons, we add artificial dissipation to cancel terms in the scheme to make it less wide, i.e. we use so called upwinding.

The dissipation operators are of a specific form and the details are given in [7]. The main properties are: $DI_p = P^{-1} R$ with $R = R^T \geqslant 0$ and DI_p approximates $d^p u / d x^p$ in the interior. At the boundary they are constructed to preserve the SBP property and thus they yield stability.

Denote by D_6 the standard difference operator approximating the sixth derivative, i.e. $D_6 = [-1, 6, -15, 20, -15, 6, -1]/h^6$. Correspondingly $D_8 = [1, -8, 28, -56, 70, -56, 28, -8, 1]/h^8$ in the interior.

The eighth-order internal scheme approximating the first derivative is, $[1/280, -4/105, 1/5, -4/5, 0, 4/5, -1/5, 4/105, -1/280]/h$. Then, for the case with an interior accuracy of order eight, we add $DI_8 = h^7 D_8/280$ and $DI_6 = h^5 D_6/105$ in the interior and thereby cancel two terms. The interior accuracy is then reduced to fifth order and the operator is only one element wider than the optimal fifth order accurate upwind operator based on block norms. Thus the loss of efficiency using diagonal norm schemes are, for upwind operators, only minor. For the construction of the full dissipation operators including the boundary we refer to [7]. We also construct downwind operators in the same manner.

Remark. The above described technique to cancel two terms in the interior is the optimal case. Sometimes that amount of dissipation is not sufficient, forcing us to increase DI_6 somewhat. That means that only one point in the stencil is cancelled, but it is still fifth-order accurate.

Remark. The same technique can be used to construct other upwind operators as well. For example, a third order upwind scheme can be constructed from the third order accurate diagonal norm scheme. Block norm schemes can of course also be used as a basis for the construction of different upwind schemes. As long as the dissipation operators of [7] are used, they will be energy stable.

3.3. The Numerical Scheme

Postponing the boundary treatment we now have the tools to discretize (2) in space. To describe the scheme we use the following notation:

$$A \otimes B = \begin{bmatrix} a_{0,0} B & \cdots & a_{0,q-1} B \\ \vdots & & \vdots \\ a_{p-1,0} B & \cdots & a_{p-1,q-1} B \end{bmatrix},$$

where A is a $p \times q$ matrix and B a $m \times n$ matrix. The $p \times q$ block matrix $A \otimes B$ is called a *Kronecker product*. There are some useful rules for Kronecker products. In this paper we will use $(A \otimes B)(C \otimes D) = (AC) \otimes (BD)$ and $(A \otimes B)^T = A^T \otimes B^T$.

Consider the domain $(a \leqslant x \leqslant b, c \leqslant y \leqslant d)$ with an $N+1 \times M+1$-points equidistant grid. That is,

$$x_i = a + i h_x, \qquad i = 0, 1, \ldots, N, \quad h_x = \frac{b-a}{N}, \tag{11}$$

$$y_j = c + j h_y, \qquad j = 0, 1, \ldots, M, \quad h_y = \frac{c-d}{M}. \tag{12}$$

The numerical approximation at grid point x_i, y_j is a $1 \times m$-vector denoted u_{ij}. We define a discrete solution vector $u^T = [u_{11}, u_{12}, \ldots, u_{1M}, u_{21}, u_{22}, \ldots, u_{NM}]$. The basic scheme to approximate $\mathbf{u}_x$ is a non-dissipative and pth order accurate finite difference approximation $(P_x^{-1} Q_x \otimes I_M)u$. But as will be seen below, we scale the artificial dissipation to obtain an upwind scheme.

A corresponding semi-discrete approximation of (2) can be written

$$
\begin{aligned}
u_t = & -(D_{+x} \otimes I_M \otimes \mathbf{A}_+)u - (D_{-x} \otimes I_M \otimes \mathbf{A}_-)u \\
& -(I_N \otimes D_{+y} \otimes \mathbf{B}_+)u - (I_N \otimes D_{-y} \otimes \mathbf{B}_-)u \\
= & -(P_x^{-1} Q_x \otimes I_M \otimes \mathbf{A})u - \alpha\,(P_x^{-1} R_x \otimes I_M \otimes I_m)u \\
& -(I_N \otimes P_y^{-1} Q_y \otimes \mathbf{B})u - \beta\,(I_N \otimes P_y^{-1} R_y \otimes I_m)u.
\end{aligned}
\tag{13}
$$

α and β are the scalings of the artificial dissipation required for the upwind formulation. Also, $D_{\pm x} = P_x^{-1}(Q_x \pm R_x)$ and similarly for $D_{\pm y}$.

3.4. Stable Interface Treatment

As an example of the block interface procedure we will consider,

$$
\mathbf{u}_t + \mathbf{A}\mathbf{u}_x + \mathbf{B}\mathbf{u}_y = 0, \quad -1 \leqslant x \leqslant 0, \ \ 0 \leqslant y \leqslant 1, \tag{14}
$$

$$
\mathbf{v}_t + \mathbf{A}\mathbf{v}_x + \mathbf{B}\mathbf{v}_y = 0, \quad 0 \leqslant x \leqslant 1, \ \ 0 \leqslant y \leqslant 1. \tag{15}
$$

In order to limit the amount of algebra we assume homogeneous boundary conditions. $\mathbf{A}$ and $\mathbf{B}$ are constant symmetric matrices with m rows and columns. The matrices are split according to Sec. 2.2. The resulting matrices are denoted $\mathbf{A}_+, \mathbf{A}_-$ and $\mathbf{B}_+, \mathbf{B}_-$.

Discretize the domains with n and l points and in the x direction and k points in the y-direction and denote the $nkm \times 1$, $lkm \times 1$ vectors u and v, respectively. Note that the grid lines at the interface match. The difference operators in the x and y direction might be different in the left and right domain and are denoted D_{-x}^L, D_{+x}^L, D_{-x}^R, D_{+x}^R, D_{-y}^L, D_{+y}^L, D_{-y}^R and D_{+y}^R. Further we introduce the following simplifications, $\tilde{I}_L = I_n \otimes I_k \otimes I_m$, $\tilde{I}_R = I_l \otimes I_k \otimes I_m$, $\tilde{\Sigma}_L = I_n \otimes I_k \otimes \Sigma_L$ and $\tilde{\Sigma}_R = I_l \otimes I_k \otimes \Sigma_R$. By using these notations, the semi-discrete system becomes,

$$
\begin{aligned}
\tilde{I}_L u_t + & (D_{+x}^L \otimes I_k \otimes \mathbf{A}_+)u + (D_{-x}^L \otimes I_k \otimes \mathbf{A}_-)u \\
& + (I_n \otimes D_{+y}^L \otimes \mathbf{B}_+)u + (I_n \otimes D_{-y}^L \otimes \mathbf{B}_-)u \\
= & ((P_x^L)^{-1} \otimes I_k \otimes I_m)\tilde{\Sigma}_L(e_N \otimes (u_N - v_0)) \\
& + \text{SAT}(x = -1, y = 0, y = 1),
\end{aligned}
\tag{16}
$$

$$\tilde{I}_R v_t + (D^R_{+x} \otimes I_k \otimes \mathbf{A}_+) v + (D^R_{-x} \otimes I_k \otimes \mathbf{A}_-) v$$
$$+ (I_l \otimes D^R_{+y} \otimes \mathbf{B}_+) v + (I_l \otimes D^R_{-y} \otimes \mathbf{B}_-) v \tag{17}$$
$$= ((P^R_x)^{-1} \otimes I_k \otimes I_m) \tilde{\Sigma}_R (e_0 \otimes (v_0 - u_N))$$
$$+ \mathrm{SAT}(x=1, y=0, y=1),$$

where the right-hand sides are the SAT penalty terms. Σ_R and Σ_L are unknown $m \times m$ matrices to be determined below by requiring stability. The term $\mathrm{SAT}(x=-1, y=0, y=1)$ and $\mathrm{SAT}(x=1, y=0, y=1)$ denotes the penalty terms at the outer boundaries. These are scaled to precisely cancel the boundary terms (see [8–11] for details). $e_0 = (1, 0, \ldots, 0)^T$ and $e_N = (0, \ldots, 0, 1)^T$ are $l \times 1$ and $n \times 1$ vectors, respectively. u_N and v_0 are $km \times 1$ vectors with components corresponding to the interface points. Define the norms $M_L = (P^L_x \otimes P^L_y \otimes I_m)$ and $M_R = (P^R_x \otimes P^R_y \otimes I_m)$. Apply the energy method by multiplying (16) and (17) by $u^T M_L$ and $v^T M_R$, respectively. Let $\tilde{R}^{L,R}_y = P^{L,R}_x \otimes R^{L,R}_y \otimes I_m$ and $\tilde{R}^{L,R}_x = R^{L,R}_x \otimes P^{L,R}_y \otimes I_m$. Adding the equations to their transposes, using $Q + Q^T = B$ and assuming that $P^L_y = P^R_y = P_y$ yield,

$$\frac{d}{dt}(\|u\|^2_{M_L} + \|v\|^2_{M_R}) = (u_N \ v_0) P_y \otimes \mathbf{M} (u_N \ v_0)^T$$
$$- 2 (u \ v) \mathbf{R} (u \ v)^T. \tag{18}$$

Note that the boundary terms at the outer boundaries are cancelled by the SAT terms. In (18), $\mathbf{R} = \mathrm{diag}(\alpha_L \tilde{R}^L_x + \beta_L \tilde{R}^L_y, \alpha_R \tilde{R}^R_x + \beta_R \tilde{R}^R_y)$ is symmetric and positive semi-definite and

$$\mathbf{M} = \begin{pmatrix} -\mathbf{A} + 2\Sigma_L & -\Sigma_L - \Sigma_R \\ -\Sigma_L - \Sigma_R & \mathbf{A} + 2\Sigma_R \end{pmatrix}.$$

To obtain stability $\mathbf{M}$ has to be negative semi-definite which is achieved by choosing Σ_L and Σ_R properly.

Since A is a symmetric matrix we can diagonalize it by $X^T A X = \Lambda$, where X is a matrix consisting of the eigenvectors of A. Further, consider penalty parameters Σ_L and Σ_R of the form $X^T \Sigma_L X = \Lambda_L$ and $X^T \Sigma_R X = \Lambda_R$. Denote by λ^i the ith diagonal component of Λ and similarly λ^i_L and λ^i_R for Λ_L and Λ_R. Then we obtain for $i = 1 \ldots m$,

$$\lambda^i_L < \frac{\lambda^i}{2}, \tag{19}$$

$$\lambda^i_R = \lambda^i_L - \lambda^i. \tag{20}$$

(The details can be found in [1].) Equation (19) is the stability condition and (20) is recognized as the conservation condition, (see for example [9]).

With Λ_L and Λ_R determined, inserting $\Sigma_L = X \Lambda_L X^T$ and $\Sigma_R = X \Lambda_R X^T$ in (16) and (17) yields a stable scheme.

Remark. As an example of the SAT terms for the outer boundaries we give the penalty term at $x = -1$ which would be included in SAT$(x = -1, y = 0, y = 1)$. It is

$$((P_x^L)^{-1} \otimes I_k \otimes \Sigma_{L,-1}) e_0 \otimes (u - g),$$

where the vector g holds the boundary data and $\Sigma_{L,-1}$ is the penalty matrix. Denote by $\Lambda^{+,-}$ the diagonal matrix holding the positive and negative eigenvalues of A such that $\Lambda^+ + \Lambda^- = \Lambda = X^T A X$. For stability, $X^T \Sigma_{L,-1} X = \Sigma^d$ must satisfy $2\Sigma^d + \Lambda^+ \leqslant 0$, i.e. $\lambda_i^+ + 2\sigma_i \leqslant 0$.

Remark. The technique of splitting the domain into blocks not only simplifies grid generation but also allows for an efficient parallelization since only the interface points have to be shared.

3.5. Reducing Spectral Radius of $P^{-1}Q$

In order to speed up convergence to steady state it is essential that the spectral radius of the numerical scheme is minimal. In [12], analytical expressions for the first derivative SBP operators of different orders are derived. The free parameters remaining in the operators to close the expressions are in [12] chosen to give the minimal width of the operator near the boundary. However, it is more important to have operators with small spectral radius such that a larger time step may be used. In particular when explicit time stepping is performed. Thus, we have searched the parameter space to find a better choice and indeed it is possible to severly reduce the spectral radius. In Appendix A in [12] the parameters x_1, x_2, and x_3 for the fifth order diagonal norm scheme are chosen,

$$x_1 = 1714837/4354560 \approx 0.394,$$
$$x_2 = -1022551/30481920 \approx -0.034,$$
$$x_3 = 6445687/8709120 \approx 0.740,$$

to obtain a minimal bandwidth. In our case we choose,

$$x_1 = 0.649,$$
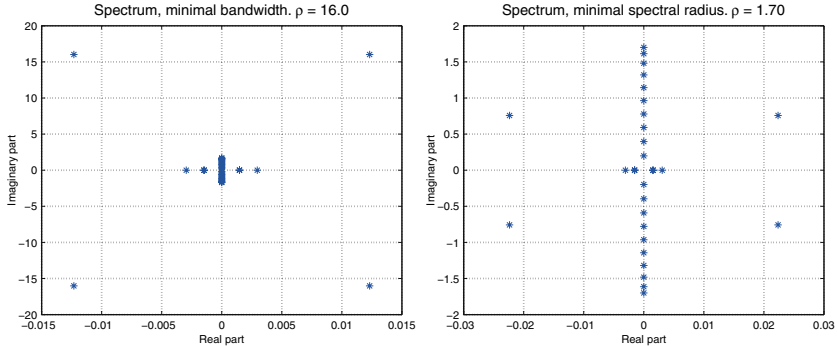$$x_2 = -0.104,$$
$$x_3 = 0.755,$$

Fig. 1. *Left:* Spectrum of original fifth-order accurate SBP operator. *Right:* Spectrum of modified fifth-order accurate SBP operator.

and obtain a much smaller spectral radius. For simplicity, we will use the term spectrally optimized to denote the operator with reduced spectral radius though we do not claim that we have found a formal extremum.

In Fig. 1, the spectrum of the original fifth order diagonal norm operator is shown as well as the corresonding data for the modified operator. The spectral radii differs by a factor of approximately 9.4. To test the effect of the reduction of the spectral radius we consider the following system of equations:

$$u_t + u_x = 0, \ \ u(0) = v(0), \tag{21}$$

$$v_t - v_x = 0, \ \ v(1) = v(1). \tag{22}$$

The system is discretized using the spectrally and non-spectrally optimized operators and a fourth order Runge–Kutta discretization in time. The largest possible quotient $CFL = \Delta t / \Delta x$ was deduced experimentally and found to be $CFL_{\text{opt}} = 1.65$ and $CFL_{\text{nonopt}} = 0.176$, that is approximately a factor 9.4. This corresponds well to the spectra of the two different discretizations (see Fig. 2). Further, note that in Fig. 2 the eigenvalues are located only in the left halfplane.

As dissipation is added to construct an upwind operator, the spectrum is altered. But it only seems to give a small perturbation of the original spectrum and CFL number.

Note also, that the originally large spectral radius of the SBP-operator is not typical and is due to the boundary closure that ensures the SBP-property. Other boundary schemes may have smaller spectral radii but they are not necessarily energy stable (see for example [13]).
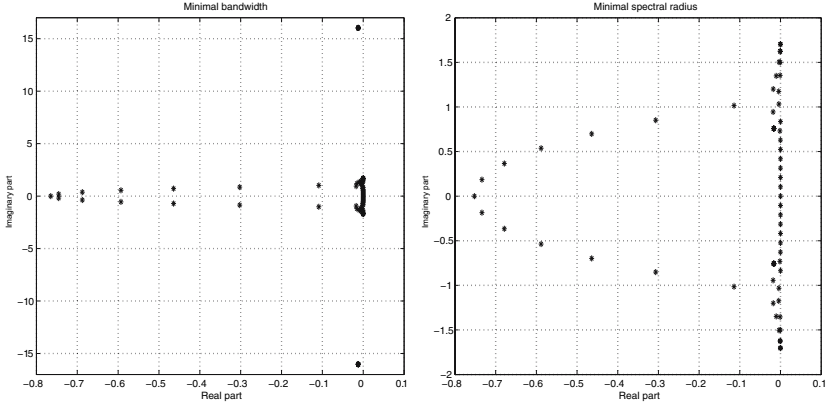
Fig. 2. Spectra of the discretized problem (21) and (22). *Left:* Original fifth-order accurate SBP operator. *Right:* Modified fifth-order accurate SBP operator.
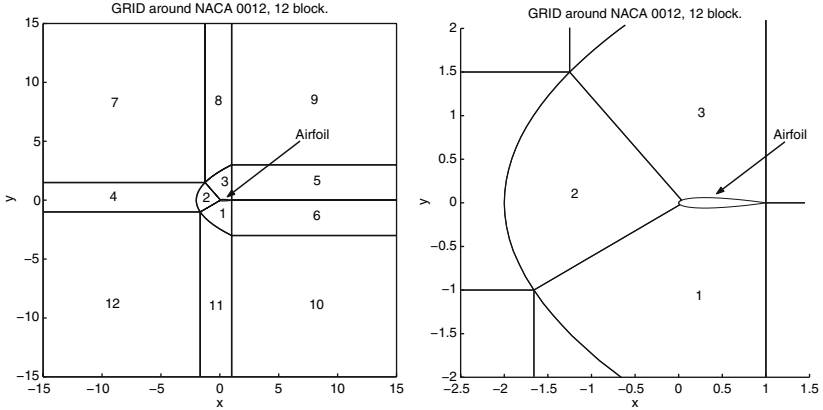

Fig. 3. The computational domain around a NACA0012 airfoil divided into 12 blocks. The right subfigure is a close up.

4. NUMERICAL COMPUTATIONS

Next, we consider steady state calculations around NACA0012 at 2 degrees angle of attack and Mach-number (Ma) 0.63. The solution will be calculated using a second and fifth order scheme. The blocking of the grid is shown in Fig. 3. The solution is considered to have reached steady state when the residual is less than 10^{-12}.

The total amount of grid points and the number of points resolving the airfoil is given in Table I.

Table I. The Total Number of Points in Different Grids and the Resolution of the Airfoil

Grid	Total	Airfoil
1	18600	140
2	74400	280

4.1. Convergence to Steady State

To investigate the effect of non-energy stable schemes we have computed solutions with the stable fifth-order scheme and also with a fifth-order block norm scheme (see [12]). The last scheme is not formally stable on the grid since the grid is curvilinear. On both Grid 1 and Grid 2 we compute solutions with the fifth order diagonal and block norm schemes. We alter the amount of dissipation, that is the constant c in front of D_6 described in Sec. 3.2. To cancel a second point in the original scheme, we must chose $c = h^5/(105)$. That is, however, a too small dissipation. We begin with a small dissipation and increase it to investigate the behavior of the schemes. All the computations are made with a constant small time step. The results are presented in Table II. Figure 4 shows a typical convergence history when the diagonal norm scheme converges and the block norm scheme levels out.

Although it is possible to obtain convergence for both schemes the block norm scheme requires significantly more artificial dissipation. That in turn, results in a larger spectral radius for the difference operators and hence a need for smaller time steps.

In [6] it is shown for a linear equation with zero growth rate that small positive eigenvalues are obtained when using a block norm scheme. Probably, this is the case in the above computations in a non-linear sense. However, with sufficient artificial dissipation the block norm scheme can be made converegent. The reason that the computations do not explode is probably due to the non-linearity. When the residual decreases, the solution is close to stationary and the Jacobian of the fluxes is locally approximately constant. Hence, the linear theory applies and we obtain a growth. However, as the growth become significant the conditions changes and linear theory is no longer relevant.

Note that even the non-energy stable scheme is stable for all cases where the diagonal norm scheme is stable. That is, in the sense that the solutions do not explode. In fact there are several notions of stability. According to the definitions in [14], stability only means boundedness of

Table II. Behavior of Block and Diagonal Norm Schemes for Different Amount of Artificial Dissipation

Scheme/grid	$c = h^5/30$	$c = h^5/20$	$c = h^5/15$	$c = h^5/10$
Block/2	Unstable	Levels out	Turns up and levels out	Converges
Diagonal/2	Turns up and levels out	Converges	Converges	Converges
Block/1	Unstable	Unstable	Turns up and levels out	Levels out
Diagonal/1	Unstable	Unstable	Turns up and levels out	Converges

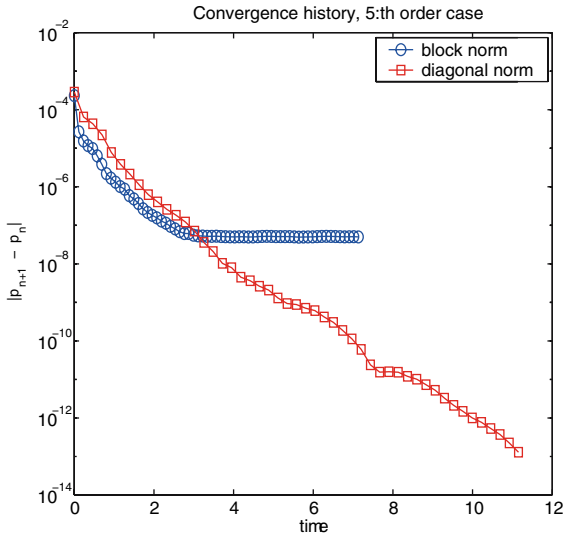The descriptions refer to the residual between two consecutive time steps.

Fig. 4. Steady-state convergence for fifth order diagonal and block norm scheme on Grid 1.

the growth of the solution. This does not implicate that the time growth of the discrete problem on a fine mesh is the same as for the continuous. This means that it may be impossible to drive the convergence to steady state arbitrary far. However, if the scheme is strictly stable it means that the time growth converges to the correct growth rate, i.e. for a given residual we can grid refine in space until that demand is fulfilled. Neither of these

stability notions are appropriate for steady-state calculations since we can in general not afford such grid refinements but want to design the grid only to resolve the expected solution well. Rather, we would like to compute a solution arbitrary close to steady state for a given grid. The energy stable diagonal norm schemes do fulfill this requirement.

Remark. Note that the non-energy stable scheme is stable in the von Neumann sense, i.e. it is stable for the Cauchy problem, even for curvilinear grids. This indicates that the instability is triggered by the boundary treatment only.

Next, we will compare the maximum time step possible for the fifth-order energy stable non-spectrally and spectrally optimized SBP operators. Also in the airfoil computations the timestep could be increased to the same order of magnitude as for the model equation in Sec. 3.5. In this case we gained a factor 9. Of course, the same factor reduces the time to reach steady state. In fact, the timestep can be taken almost as large for the fifth-order scheme as for the second order scheme. The difference is approximately 20% which also is the difference in the number of iterations to reach steady state. The second order scheme use a fourth-order artificial dissipation and is thus 5 points wide and the fifth-order scheme is 7 (or 8) points wide. Together with the 20% difference in the time step we obtain approximately a factor 2 for the difference in efficiency of the two schemes.

Figure 5 shows a typical solution on Grid 2. The figure is a blow up around the leading edge to better show the stuctures of the flow. Note the smoothness across the block interfaces.

4.2. Spectra of Different Stencils

The first test of whether a scheme is suitable for the Euler equations is usually the advection equation. However, the advection equation only mimics the supersonic Euler equations in that it transports the solution out through the boundary. The subsonic Euler equations with a pressure boundary condition at the outflow boundary couple the characteristics in such a way that a part of the solution is fed back into the domain. The systems (21) and (22) models that behavior, though it might be even more sensitive to stability problems than the Euler equations since energy never leaves the system.

To further investigate the expected growth of the solution for different stencils, we will consider the systems (21) and (22) discretized by two different stencils: the internally sixth order accurate with fifth order boundary closure block norm SBP-scheme, i.e. the basis for the upwind block norm
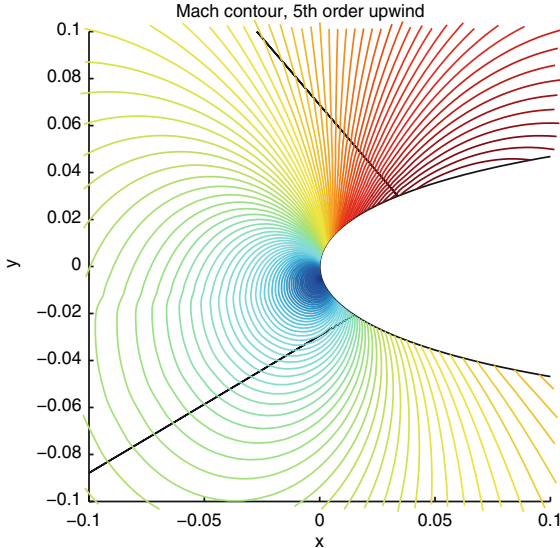
Fig. 5. Steady-state solution for the fifth order scheme on grid 2. Contour plot of the Mach-number.

operator used throughout the article; and the same internally sixth order accurate scheme with the fifth order boundary closure proposed in [13]. The last one will be called the non-SBP scheme. In [13] a spectrum for the non-SBP scheme applied to the advection equation was computed showing stability for that equation. Further, the non-SBP scheme is succesfully used in [15] for Maxwell's equations. We will not consider the fifth order diagonal norm scheme since it can be proven strictly dissipative.

We apply these schemes to the systems (21) and (22) with two different grid spacings. One is an equidistant grid spacing and the other is a slightly stretched grid. The stretching between two adjacent cells ranges between 3 and 6%. The spectra for the block norm SBP-scheme is seen in Fig. 6 and for the non-SBP scheme in Fig. 7. The block norm SBP scheme do not have positive eigenvalues in the equidistant case. But in the non-equidistant case there are small positive eigenvalues. The non-SBP scheme have positive eigenvalues in both the equidistant and non-equidistant case.

Both the schemes have identical non-dissipative central difference stencils in the interior. When computing solutions to the Euler equations artificial dissipation is added. With enough dissipation, it is possible that the spectrum can be adjusted such that no positive eigenvalues exist. However, this also leads to large negative eigenvalues which have a negative effect on
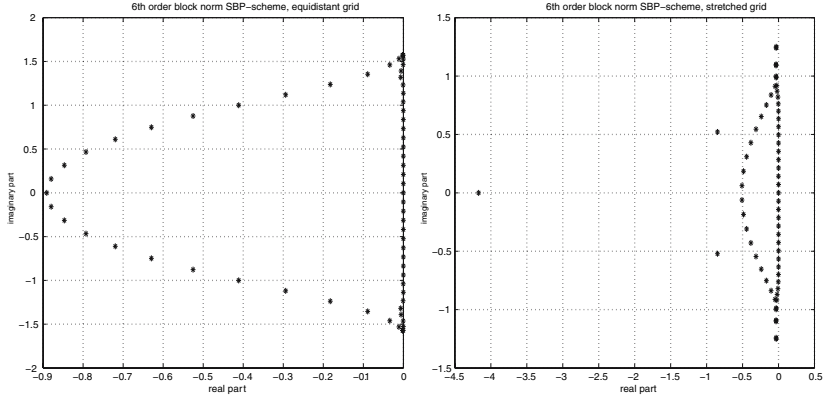
Fig. 6. Spectrum of the discretized problem (21) and (22). *Left:* The block norm SBP scheme on equidistant grid. Maximum real part, -1×10^{-16} *Right:* The block norm SBP scheme on a stretched grid. Maximum real part, 4.5×10^{-4}.
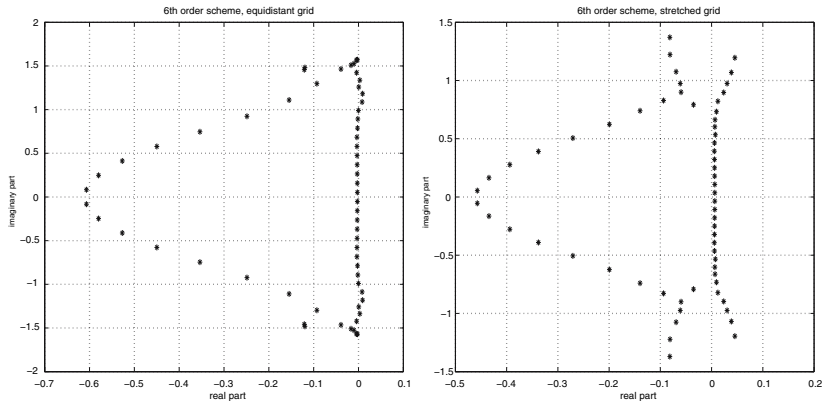

Fig. 7. Spectrum of the discretized problem (21) and (22). *Left:* The 6th order non-SBP scheme on equidistant grid. Maximum real part, 0.0092 *Right:* The sixth order non-SBP scheme on a stretched grid. Maximum real part, 0.0454.

the time step in case of explicit time stepping. Furthermore, the accuracy of the solution decreases with increasing amount of dissipation.

5. CONCLUSIONS

We have given numerical evidence that energy stability is important when computing steady state solutions to partial differential equations. On curvilinear grids the SBP block norm schemes are not energy stable as is

shown in [6] and accordingly they might yield small positive eigenvalues that destroy convergence to steady state. However, for the diagonal norm scheme no such behavior is observed and in that case stability proofs using the energy method are obtainable.

Furthermore, we have given improvement of the difference operators such that a considerably larger time step may be used. This contributes to a fast convergence to steady state.

REFERENCES

1. Mattsson, K., Svärd, M., Nordström, J., and Carpenter, M. H. (2003). Accuracy Requirements for Transient Aerodynamics *AIAA paper* 2003–3689.
2. Zingg, D. W. (2000) Comparison of high-accuracy finite-difference methods for linear wave propagation. *SIAM J. Sci. Comput.* **22**, 476–502.
3. Zingg, D. W., De Rango, S., Memec, M., and Pulliam, T. H. (2000). Comparison of Several Spatial Discretizations for the Navier-Stokes equations. *J. Comput. Phys.* **160**, 683–704.
4. Kreiss, H.-O., and Scherer, G. (1974). Finite element and finite difference methods for hyperbolic partial differential equations. *Mathematical Aspects of Finite Elements in Partial Differential Equations,* Academic Press Inc. New York.
5. Kreiss, H.-O. and Scherer, G. (1977). On the existence of energy estimates for difference approximations for hyperbolic systems Technical report, Dept. of Scientific Computing Uppsala University.
6. Svärd, M. (2004). On coordinate transformations for summation-by-parts operators. *J. Sci. Comput.* **20**(1), 29–42.
7. Mattsson, K., Svärd, M. and Nordström, J. (2004). Stable and Accurate Artificial Dissipation. *J. Sci. Comput.* **21**(1), 57–79.
8. Carpenter, M. H., Gottlieb, D., and Abarbanel, S. (1994). The stability of numerical boundary treatments for compact high-order finite-difference schemes. *J. Comput. Phys.* **108**(2), 272–295.
9. Carpenter, M. H., Nordström, J. and Gottlieb, D. (1999). A Stable and Conservative interface treatment of Arbitrary Spatial Accuracy. *J. Comput. Phys.* **148**, 341–365.
10. Nordström, J., and Carpenter, M. H. (1999) Boundary and interface conditions for high order finite difference methods applied to the Euler and Navier–Stokes equations *J. Comput. Phys.* **148**, 621–645.
11. Nordström, J. and Carpenter, M. H. (2001). High-order finite difference methods multi-dimensional linear problems and curvilinear coordinates. *J. Comput. Phys.* **173**, 149–174.
12. Strand, B. (1994). Summation by parts for finite difference approximations for d/dx. *J. Comput. Phys.* **110**, 46–67.
13. Zingg, D. W. (1997). Aspect of linear stability amalysis for higher-order finite-difference methods. *AIAA paper 1997–1939*.
14. Gustafsson, B., Kreiss, H.-O., and Oliger, J., (1995). *Time Dependent Problems and Difference Methods*. Wiley, New York.
15. Jurgens, H. M., and Zingg, D. W. (2000). Numerical solution of the time-domain maxwell equation using high-accuracy finite-difference methods. *SIAM J. Sci. Comput.* **22**, 1675–1696.